Inorganica Chimica Acta 469 (2018) 1–10

Contents lists available at ScienceDirect

Inorganica Chimica Acta

journal homepage: www.elsevier.com/locate/ica

Research paper

The complex-in-a-complex cation $[Pt(acac)_2\subset(p\text{-cym})_6Ru_6(tpt)_2(dhnq)_3]^{6+}$: Its stability towards biological ligands

Lydia E.H. Paul [a], Bruno Therrien [b], Julien Furrer [a,*]

[a] Departement für Chemie und Biochemie, Universität Bern, Freiestrasse 3, CH-3012 Bern, Switzerland
[b] Institut de Chimie, Université de Neuchâtel, Avenue de Bellevaux 51, CH-2000 Neuchâtel, Switzerland

ARTICLE INFO

Article history:
Received 16 August 2017
Accepted 21 August 2017
Available online 31 August 2017

Keywords:
Arene ruthenium
Metallaprism
Cytotoxicity
Biological ligands
Encapsulation
Drug delivery

ABSTRACT

The reactivity of the highly cytotoxic complex-in-a-complex cation $[Pt(acac)_2\subset(p\text{-cym})_6Ru_6(tpt)_2(dhnq)_3]^{6+}$ ($[Pt(acac)_2\subset\mathbf{1}]^{6+}$) towards amino acids, proteins, nucleotides and an oligonucleotide was investigated by NMR, MS, UV/Vis and CD experiments. The similarities and differences between the metallaprism $[Pt(acac)_2\subset\mathbf{1}]^{6+}$, its empty counterpart $[\mathbf{1}]^{6+}$ and the previously reported smaller complex-in-a-complex cation $[Pt(acac)_2\subset(p\text{-cym})_6Ru_6(tpt)_2(dhbq)_3]^{6+}$ ($[Pt(acac)_2\subset\mathbf{2}]^{6+}$) were described. The reactivity of $[Pt(acac)_2\subset\mathbf{1}]^{6+}$ towards amino acids and the degradation products formed were similar to those observed with $[\mathbf{1}]^{6+}$ and $[Pt(acac)_2\subset\mathbf{2}]^{6+}$ but the kinetic of the reactions was much slower. Interestingly, $[Pt(acac)_2\subset\mathbf{1}]^{6+}$ imposed stronger structural effects on the human proteins HsA, Tf, Mb, Cyt c, and Ub compared to the empty metallaprism $[\mathbf{1}]^{6+}$. The effects were similar to those of $[Pt(acac)_2\subset\mathbf{2}]^{6+}$. Unlike $[Pt(acac)_2\subset\mathbf{2}]^{6+}$ and as observed previously with $[\mathbf{1}]^{6+}$, $[Pt(acac)_2\subset\mathbf{1}]^{6+}$ did not react with nucleotides. However, similar interactions with a double stranded oligonucleotide were observed in the presence of both metallaprisms $[Pt(acac)_2\subset\mathbf{1}]^{6+}$ and $[\mathbf{1}]^{6+}$. In solution, $[Pt(acac)_2\subset\mathbf{1}]^{6+}$ disassembles at a lower rate than $[Pt(acac)_2\subset\mathbf{2}]^{6+}$. Overall, the results show that the enhanced stability of $[\mathbf{1}]^{6+}$ is kept when a guest is trapped inside the hydrophobic cavity, suggesting that the half-life of $[Pt(acac)_2\subset\mathbf{1}]^{6+}$ in the blood is probably sufficiently long to enter cells and reach the target intact.

1. Introduction

Metal ions play an important role in biological processes and are also abundantly used in diagnoses and therapies [1,2]. Since the fortuitous discovery of the cytotoxic effects of platinum compounds by Rosenberg more than fifty years ago [3], a lot of research effort was put into the development of new inorganic and organometallic compounds as anticancer drugs [4]. Although platinum drugs are still used today in more than 50% of all cancer treatments [5], their anticancer properties are counterbalanced by severe side effects and intrinsic or acquired resistances [6]. Among the new inorganic and organometallic compounds developed as potential anticancer drugs, ruthenium derivatives appear as the most prominent ones [7–9]. Eventually, this led to the discovery of two ruthenium(III) complexes, NAMI-A [10,11] and KP1019 [12], that showed very promising results in clinical trials (Chart 1). The sodium salt of KP1019, NKP-1339, takes advantage of the increased water solubility and is currently at the edge of clinical applications [13]. Considerable interest was also given to half-sandwich ruthenium(II) complexes as they also proved to be highly cytotoxic [9,14]. The RAPTA family, RM175 [15] and DW1/2 [16] are the most prominent examples [17] and also show very promising results in preclinical trials (Chart 1).

A major issue related to almost all metal-based drugs is their poor water solubility [18], which increases the risk that the compounds do not cross cell membranes and remain stacked into the lipid bilayers. Among the numerous strategies that have been developed to overcome this limitation, the use of specific delivery systems appears as one of the most promising method [19]. Systems such as nanoparticles [20], micelles [21], microspheres [22], liposomes [23], metal organic frameworks [24], dendrimers [25], organic macrocycles [26] or carbon nanotubes [27,28] can potentially host metal-based drugs, transport them into cancer cells, and eventually deliver them after internalization.

Metalla-assemblies can also be successfully used as drug delivery systems. The field of coordination-driven self-assembly

Abbreviations: AA, amino acid; dhbq, 2,5-dihydroxy-1,4-benzoquinonato; dhnq, 5,8-dihydroxy-1,4-naphthoquinonato; DOSY, diffusion-ordered spectroscopy; ESI, electrospray ionization; oxa, oxalato; tpt, 2,4,6-tri(pyridin-4-yl)-1,3,5-triazine.

* Corresponding author.
E-mail address: julien.furrer@dcb.unibe.ch (J. Furrer).

http://dx.doi.org/10.1016/j.ica.2017.08.045
0020-1693/

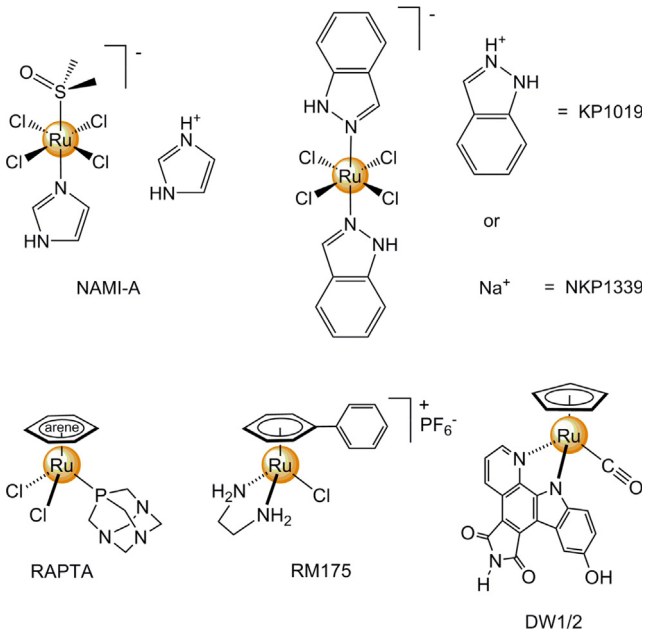

Chart 1. Molecular structures of NAMI-A, KP1019, NKP-1339, RAPTA, RM-175, and DW1/2.

was pioneered by Fujita and Stang who synthesized numerous Pd(II) and Pt(II) assemblies [29–31]. Many different metal ions can be used as building atoms for these assemblies, e.g. Pd, Pt, Rh, Zn, Cu, Ni, Cd and Ru, and a huge structural variety in the assemblies can be achieved [32]. Interestingly, it was found that half-sandwich organometallic complexes can also be used as versatile building blocks for the synthesis of metalla-assemblies [33]. Therrien and coworkers started working with arene ruthenium half-sandwich complexes as building blocks to design multi-cationic ruthenium metallarectangles, metallaprisms and metallacubes which, in some cases, allow for the encapsulation of various organic or metal organic complexes [34]. The relatively high positive charge of these assemblies increases their water solubility and gives way to various biological applications such as sensing or anticancer therapy [35]. The assemblies can host small planar metal complexes such as $M(acac)_2$ (M = Pt, Pd; acac = acetyl acetate) and like a "Trojan Horse" deliver the guest to cancer cells [36]. Interestingly, metalla-assemblies are intrinsically very cytotoxic and the encapsulation of the guest increases the cytotoxicity making these host-guest systems very effective drug delivery systems with potentially a dual mode of action [35,37–40].

Recently, three hexacationic hexaruthenium metallaprisms $([(p\text{-cym})_6Ru_6(tpt)_2(dhnq)_3]^{6+}$ ($[\mathbf{1}]^{6+}$), $[(p\text{-cym})_6Ru_6(tpt)_2(dhbq)_3]^{6+}$ ($[\mathbf{2}]^{6+}$), and $[(p\text{-cym})_6Ru_6(tpt)_2(oxa)_3]^{6+}$ ($[\mathbf{3}]^{6+}$) (Chart 2), were investigated for their interactions with amino acids [41–43], DNA [44] and proteins [45], in view to evaluate their stability and to understand their potential modes of action at the cellular level. Upon interaction with the basic amino acids (AA) Arg, His, and Lys, the metallaprisms disassembled and formed predominantly a degradation product of the general formula $[(p\text{-cym})Ru\text{-AA}]^+$. While the nature of the degradation product formed was identical for all metallaprisms, the kinetics of the reactions was very different and inversely proportional to the respective *in vitro* cytotoxicity [41–43]. Upon addition of nucleotides, the rapid formation of similar degradation products of the general formula $[(p\text{-cym})Ru(\text{nucleotide})]^+$ were identified with $[\mathbf{2}]^{6+}$, [43] and $[\mathbf{3}]^{6+}$, [41] but interestingly not with the most cytotoxic metallaprism $[\mathbf{1}]^{6+}$ [42], confirming the relation "high *in vitro* cytotoxicity- weak reactivity", as suggested by others [46]. Surprisingly, no covalent adducts were found in the presence of an oligonucleotide [44] or proteins [45]. However, the three metallaprisms induced severe structural changes to both oligonucleotide and proteins, due to electrostatic interactions.

Subsequently, we found that the encapsulation of $Pt(acac)_2$ increased the overall cytotoxicity of the metallaprism $[\mathbf{2}]^{6+}$ and also moderately affected its reactivity [47]. Overall, the guest molecule reduced the reaction rates for the interaction with all biomolecules and the filled metallaprism had a stronger effect on the secondary structure of proteins and oligonucleotides as compared to the empty prism [47]. However, as $[Pt(acac)_2{\subset}\mathbf{2}]^{6+}$ rapidly disassembled upon addition of large excess of Arg, His, and Lys, the half-life of the metallaprism $[\mathbf{2}]^{6+}$ in the blood is probably too short and $[\mathbf{2}]^{6+}$ is unlikely reaching its target intact. Further fine tuning of the dismantling rate of such complex-in-a-complex is therefore highly desirable. This is partly achievable by varying the structure of the metallaprism, as shown for instance for the metallaprism $[\mathbf{1}]^{6+}$ [42].

In the present study, in order to exemplify the potential of such complex-in-a-complex systems to deliver smaller metal drugs in complexed biological mixtures, we wish to present our results for the larger, more cytotoxic and more stable metallaprism $[\mathbf{1}]^{6+}$ [42], and the complex-in-a-complex system $[Pt(acac)_2{\subset}\mathbf{1}]^{6+}$ (Chart 3). The reactivity of $[Pt(acac)_2{\subset}\mathbf{1}]^{6+}$ with various biomolecules was investigated with the aim of comparing the results obtained with the empty metallaprism $[\mathbf{1}]^{6+}$ and with the smaller complex-in-a-complex $[Pt(acac)_2{\subset}\mathbf{2}]^{6+}$ [47].

2. Experimental section

2.1. Chemicals

Chemicals obtained from commercial suppliers were used as received and were of analytical grade; $RuCl_3{\cdot}nH_2O$ was obtained from Johnson Matthey; L-Arg, L-Cys, L-His and L-Lys were purchased from Acros and Glutathione from Sigma Aldrich. The proteins HsA, Tf, Mb, Ub and Cyt c and the nucleotides dAMP, dCMP, dGMP and dTMP were obtained from Sigma Aldrich. The oligonucleotide d $(CGCGATCGCG)_2$ was ordered from Microsynth AG. This dodecamer was chosen because its NMR spectrum has been completely assigned [48,49] and it forms a complete turn including a minor and a major groove in the double helix [50]. The ruthenium metallaprisms $[\mathbf{1}](CF_3SO_3)_6$, $[Pt(acac)_2{\subset}\mathbf{1}](CF_3SO_3)_6$ and $[Pt(acac)_2{\subset}\mathbf{2}](CF_3SO_3)_6$ were synthesized according to published methods [40,51].

2.2. NMR spectroscopy

2.2.1. Sample preparation

Samples containing amino acids, GSH and nucleotides were prepared by taking 50 μL of a stock solution obtained by mixing 2 mg $[Pt(acac)_2{\subset}\mathbf{1}](CF_3SO_3)_6$ in 1 mL D_2O (concentration c = 0.514 mM) with approximately 6–10 equivalents of the corresponding substrate. With proteins, $[Pt(acac)_2{\subset}\mathbf{1}](CF_3SO_3)_6$ was mixed with 0.1 equivalents of the corresponding proteins in 50 μL D_2O. For the oligonucleotide sample, a stock solution of $d(CGCGATCGCG)_2$ in D_2O (containing 0.01% NaN_3 and 10 mM Na_2HPO_4/KH_2PO_4; c = 3.575 mM) was first prepared. Afterwards, a solution of the oligonucleotide was incubated with $[Pt(acac)_2{\subset}\mathbf{1}](CF_3SO_3)_6$ at a 1:1 M ratio. All experiments were undertaken without pH control to avoid premature disassembly of $[Pt(acac)_2{\subset}\mathbf{1}]^{6+}$ due to the presence of various anions as observed previously with the empty metallaprism [42]. The reactions of $[Pt(acac)_2{\subset}\mathbf{1}]^{6+}$ with amino acids, proteins and nucleotides were performed in buffer-free solvents. The influence of pH was investigated previously and it was

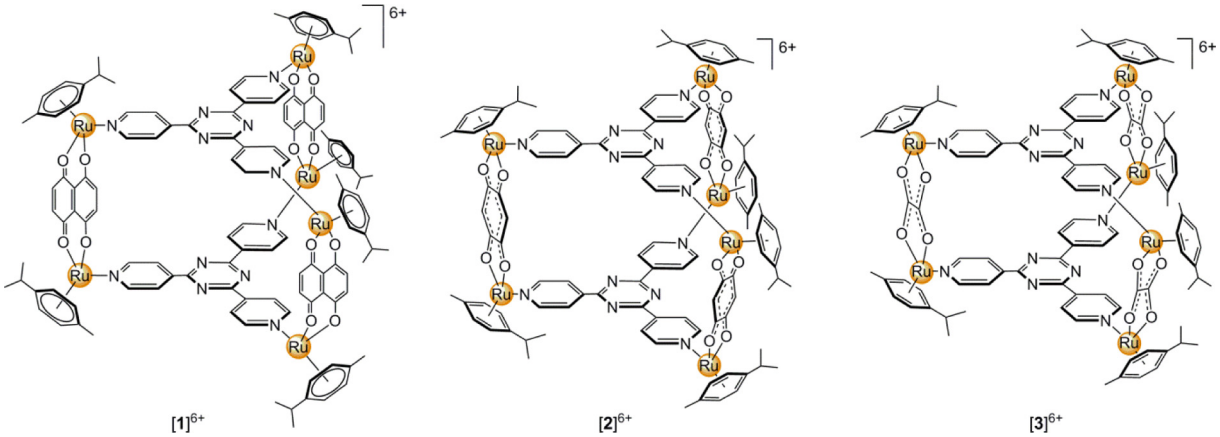

Chart 2. Hexacationic hexaruthenium metallaprisms ($[(p\text{-cym})_6Ru_6(tpt)_2(dhnq)_3]^{6+}$ ($[\mathbf{1}]^{6+}$), $[(p\text{-cym})_6Ru_6(tpt)_2(dhbq)_3]^{6+}$ ($[\mathbf{2}]^{6+}$), and $[(p\text{-cym})_6Ru_6(tpt)_2(oxa)_3]^{6+}$ ($[\mathbf{3}]^{6+}$).

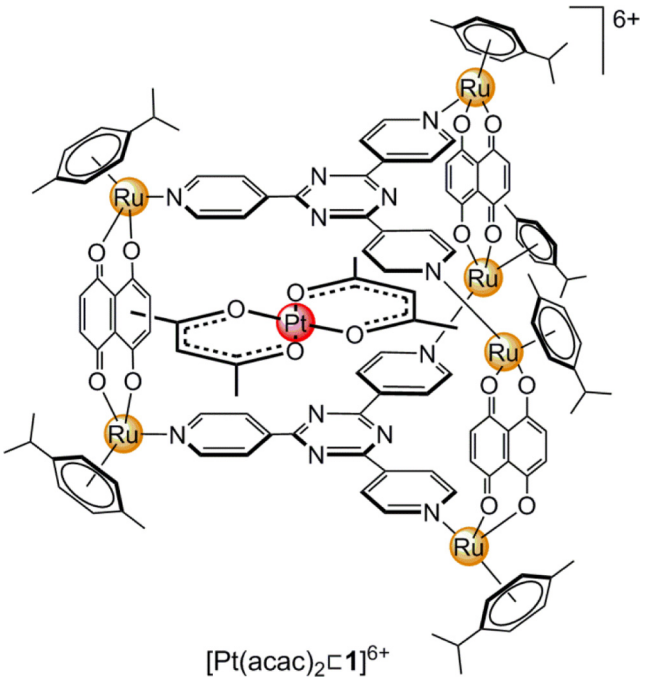

Chart 3. Hexacationic hexaruthenium complex-in-a-complex $[Pt(acac)_2\subset(p\text{-cym})_6Ru_6(tpt)_2(dhnq)_3]^{6+}$ ($[Pt(acac)_2\subset\mathbf{1}]^{6+}$).

established that the degradation products are still formed under various pH conditions [52–54]. To mimic physiological conditions as closely as possible during the experiments, oxygen was not excluded from solutions.

2.2.2. NMR experiments

For investigating the reaction of $[Pt(acac)_2\subset\mathbf{1}](CF_3SO_3)_6$ with the various biomolecules, all mixtures were first monitored by 1D ^{1}H NMR spectroscopy over a prolonged period of up to 48 h (amino acids, nucleotides), and of up to 96 h (proteins and dodecamer). The series of 2D NMR spectra were recorded subsequently.

NMR data were acquired at a regulated temperature of 37 °C using a Bruker AvanceII 500 MHz NMR spectrometer, equipped with an inverse 1.7 mm triple channel (^{1}H, ^{31}P, ^{13}C) *z*-gradient microprobehead. All samples were kept at 37 °C between the measurements. All 1D ^{1}H NMR data were measured with 64–1 k transients into 16 k–64 k data points over a width of 20 ppm using a classical presaturation to eliminate the water resonance. A relaxation delay of 5 s (amino acids and nucleotides) or 2 s (proteins and dodecamer) was applied between transients. 2D ^{1}H-DOSY NMR experiments were acquired with a standard pulsed-gradient stimulated echo (LED-PFGSTE) sequence containing bipolar gradients [55,56]. For each data set, 8 k complex points were collected. A 1s recycle delay was used between scans for data shown. The number of scans ranged from 32 to 128, and was adapted to each sample. All NMR data were processed using Topspin (Version 3.0 and 3.2, Bruker Switzerland) and Dynamics Center (Version 2.3.2, Bruker BioSpin Switzerland).

2.3. Mass spectrometry studies

2.3.1. Amino acids and GSH

Mass spectrometric analyses were performed on a LTQ Orbitrap XL mass spectrometer (Thermo Fisher Scientific, Bremen, Germany), equipped with a nanoelectrospray ion source. For the mass spectrometry studies on the binding to selected biological ligands stock solutions of the metallaprism, Arg, His, Cys, and Lys (each 0.257 mM for $[Pt(acac)_2\subset\mathbf{1}](CF_3SO_3)_6$) were prepared in H_2O. Solutions of $[Pt(acac)_2\subset\mathbf{1}](CF_3SO_3)_6$ were incubated with the selected amino acid at a 1:10 M ratio for 48 h at 37 °C, for GSH the molar ratio was 1:6. The samples were analyzed in the positive ion mode with a voltage of +700 V applied to the glass emitter (New Objective, Woburn, MA, USA). The tube lens was at +150 V and the transfer capillary was held at 200 °C. Spectra were acquired in the FTMS mode over a range from *m*/*z* 100 to 2000 with a resolution of 100,000 at *m*/*z* 400. Calibration of the instrument was performed with ProteoMass LTQ/FTHybrid ESI positive mode calibration mix (Supelco Analytical, Bellefonte, PA, USA). The Xcalibur software package (Xcalibur 2.0.7, Thermo Fisher Scientific) was used for instrument control and data processing.

2.3.2. Proteins

MALDI-TOF mass spectrometry analyses were performed on a Bruker Daltonics Autoflex III MALDI-TOF mass spectrometer equipped with a smartbeam Nd:YAG-laser (355 nm) providing a repetition rate of 200 Hz. 1 mg of $[Pt(acac)_2\subset\mathbf{1}](CF_3SO_3)_6$ dissolved in 1 mL H_2O was incubated with the selected protein at a 10:1 M ratio for 48 h at 37 °C. The samples were analyzed using various matrices depending on the protein. For HsA, Tf, Cyt c and Ub, CHCA (α-Cyano-4-hydroxycinnamic acid) was applied and for Mb an SA (sinapic acid) matrix was used. The Xcalibur software package (Xcalibur 2.0.7, Thermo Fisher Scientific) was used for instrument control and data processing. ESI mass spectrometry analyses were performed as described above for the amino acids. A molar ratio $[Pt(acac)_2\subset\mathbf{1}](CF_3SO_3)_6$: protein of 10:1 was used.

2.3.3. Nucleotides and oligonucleotide

Electrospray ionization mass spectrometry (ESI MS) analyses were performed on a LTQ Orbitrap XL mass spectrometer (Thermo Fisher Scientific, Bremen, Germany), equipped with a nanoelectrospray ion source. A solution comprising 1 mg of $[Pt(acac)_2\subset\mathbf{1}](CF_3SO_3)_6$ dissolved in 1 mL H_2O was incubated with the selected nucleotide at a 1:6 M ratio for 48 h at 37 °C. For the experiments with the oligonucleotide, $[Pt(acac)_2\subset\mathbf{1}](CF_3SO_3)_6$ was dissolved in a stock solution of the oligonucleotide in H_2O to reach a 1:1 M ratio, and incubated for 48 h at 37 °C. Subsequently, all samples were analyzed in the positive ion mode as described above.

2.4. Circular dichroism studies

2.4.1. Proteins

The circular dichroism (CD) spectra of the proteins in the presence or absence of the metallaprism were accumulated on a J-715 Jasco Spectropolarimeter (with Xe lamp, purged with nitrogen). All experiments were measured using a Hellma Suprasil R 100-QS 0.1 cm cuvette. The metallaprism $[Pt(acac)_2\subset\mathbf{1}](CF_3SO_3)_6$ and the proteins were dissolved in H_2O and incubated for 48 h before data collection. For each sample, the mixture was scanned three times using a rate of 50 nm/min at 20 °C. The range of measurement was 190 – 700 nm, pitch was 0.5 nm, response 16 s, and band 1.0 nm. The nitrogen flow was kept around 5 L/min. All spectra were corrected for solvent signal contribution and measured under identical conditions.

2.4.2. Oligonucleotide

The circular dichroism spectra of the oligonucleotide in the presence or absence of the metallaprisms were also accumulated on a J-715 Jasco Spectropolarimeter (with Xe lamp, purged with nitrogen) over a wavelength range of 700–200 nm using a Hellma Suprasil R 100-QS 0.1 cm quartz cuvette. The metallaprism $[Pt(acac)_2\subset\mathbf{1}](CF_3SO_3)_6$ was dissolved in the oligonucleotide stock solution in buffered H_2O (10 mM PBS + 0.01% NaN_3) and incubated for 0 h, 24 h and 48 h before data collection. For each sample, the mixture was scanned three times using a rate of 50 nm/min at 20 °C. The nitrogen flow was kept around 5 L/min. All spectra were corrected for buffer signal contribution and measured under identical conditions.

2.5. UV/Vis spectroscopy

All UV/Vis spectra were recorded on a Cary 100 Bio UV/Visible Spectrometer over a wavelength range of 800 – 190 nm using 1.0 cm quartz cells. The spectra were corrected for buffer signal contribution and measured under identical conditions. For the measurements, a stock solution of the oligonucleotide sample (c = 10 μM) was first prepared in buffered solution and UV/Vis spectra were recorded directly after folding of the doublestrand. The measurement was repeated after 24 h to ensure stability in solution. Afterwards, the metallaprism was dissolved in this stock solution to achieve a 1:1 M ratio. The solution was mixed properly and spectra were recorded directly thereafter and again after a 24 h incubation period.

2.6. Cell culture and inhibition of cell growth

The human ovarian carcinoma cells A2780 and the cisplatin-resistant mutant A2780cisR were obtained from the European Collection of Cell Cultures (Salisbury, UK). Cells were grown routinely in RPMI-1640 medium with 10% foetal calf serum (FCS), 2 mM Gln and 1% penicillin/streptomycin at 37 °C and 5% CO_2.

The human embryonic kidney cells HEK-293 were graciously provided by the group of Professor Reymond and routinely grown in DMEM medium with 10% foetal calf serum (FCS), 2 mM Gln, 1% HEPES buffer and 1% penicillin/streptomycin at 37 °C and 5% CO_2.

Cytotoxicity was determined using the cell counting-kit 8 (Dojindo). Cells were seeded in 96-well plates as monolayers with 100 μL of cell solution (approximately 10,000 cells) per well. Compounds were prepared as DMSO solution then dissolved in the culture medium and serially diluted to the appropriate concentration to give a final DMSO concentration of 1%. 100 μL of drug solution was added to each well and the plates were incubated for 96 h. After that the culture medium was removed completely and subsequently, 10 μL kit solution and 100 μL fresh medium were added to the cells and the plates were incubated for a further 90 min. The optical density, directly proportional to the number of surviving cells, was quantified at 450 nm using a multiwell plate reader and the fraction of surviving cells was calculated from the absorbance of untreated control cells. Evaluation is based on means from four independent experiments, each comprising four microcultures per concentration level.

3. Results and discussion

3.1. Stability in aqueous solution

The stability of the complex-in-a-complex $[Pt(acac)_2\subset\mathbf{1}]^{6+}$ in D_2O at 37 °C was assessed by ^1H NMR spectroscopy over 24 h (Fig. 1). No additional resonances or significant chemical shift changes were observed indicating that $[Pt(acac)_2\subset\mathbf{1}]^{6+}$ is stable in water for at least 24 h, and that $Pt(acac)_2$ remains encapsulated in the cavity. As such, $[Pt(acac)_2\subset\mathbf{1}]^{6+}$ is equally stable in water than the related complex-in-a-complex $[Pt(acac)_2\subset\mathbf{2}]^{6+}$ [47] and the empty metallaprism $[\mathbf{1}]^{6+}$ [42].

3.2. Reaction with amino acids

Similarly to the results obtained with $[\mathbf{1}]^{6+}$ [42], $[\mathbf{2}]^{6+}$ [43], and $[Pt(acac)_2\subset\mathbf{2}]^{6+}$ [47], the ^1H NMR spectra of the mixture $[Pt(acac)_2\subset\mathbf{1}]^{6+}$/Arg (ratio 1:10) recorded between t = 5 min and t = 24 h show the gradual disappearance of the resonances of the tpt and dhnq moieties between 7 and 8 ppm and of $Pt(acac)_2$ between 0 and 4 ppm (Fig. 2). This indicates that $[\mathbf{1}]^{6+}$ slowly disassembled in solution, and that $Pt(acac)_2$ is presumably released and precipitates due to its low solubility in water. Simultaneously, new resonances adjacent to the resonances of free Arg (δ = 1.75, 3.33 and 3.42 ppm) and to the resonances of *p*-cym (δ = 5.71 and 6.00 ppm) have progressively appeared, indicating that at least one degradation product is formed where Arg presumably acts as chelating ligand for the (*p*-cym)Ru moiety. The same observation was made for $[\mathbf{1}]^{6+}$ [42] and $[\mathbf{2}]^{6+}$ [43] and for other arene ruthenium complexes [46,54,57]. The 2D ^1H-DOSY NMR spectrum of the mixture recorded 24 h after reaction time supports these findings (Fig. S1): Two different species with distinct diffusion coefficients are present in solution: One species with the largest diffusion coefficient can be assigned to the plausible degradation product $[(p\text{-cym})Ru(Arg)]^+$, and the second one with the smallest diffusion coefficient to free Arg. The DOSY NMR spectrum of $[\mathbf{1}]^{6+}$ has been superimposed for comparison. Clearly, no resonances of $[\mathbf{1}]^{6+}$ are visible in the DOSY spectrum of the mixture $[Pt(acac)_2\subset\mathbf{1}]^{6+}$/Arg, indicating that $[Pt(acac)_2\subset\mathbf{1}]^{6+}$ reacted completely after 24 h.

The kinetic of reaction with Arg is however slower than the empty metallaprism $[\mathbf{1}]^{6+}$: The reaction of Arg with $[\mathbf{1}]^{6+}$ was already substantial 10 min after sample preparation (Fig. S2). The same tendency was assumed with the smallest metallaprisms $[Pt(acac)_2\subset\mathbf{2}]^{6+}$ and $[\mathbf{2}]^{6+}$, albeit the dismantling was almost instantaneous in both cases [42,47].

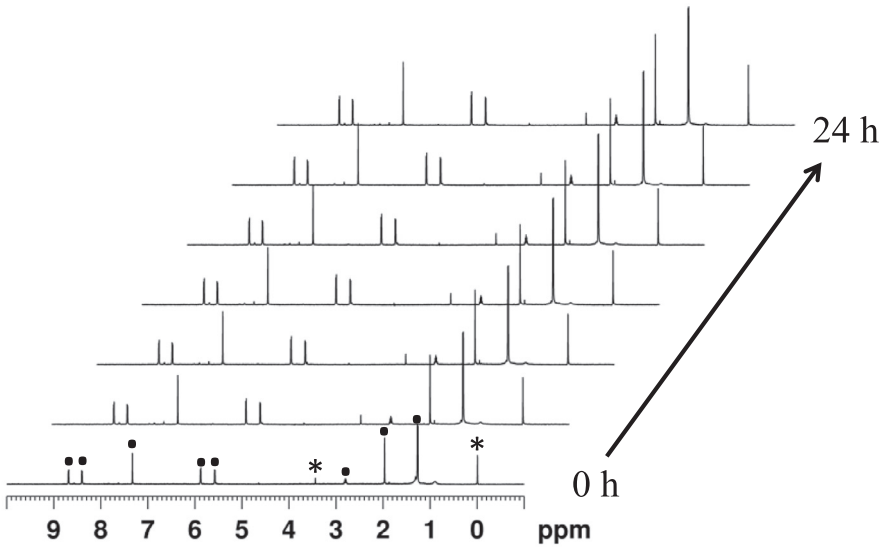

Fig. 1. Stability of $[Pt(acac)_2 \subset \mathbf{1}]^{6+}$ in D_2O (37 °C) monitored by ^1H NMR spectroscopy during 24 h. The resonances of the metallaprism $[\mathbf{1}]^{6+}$ are marked with (•) and the resonances of $Pt(acac)_2$ with (*).

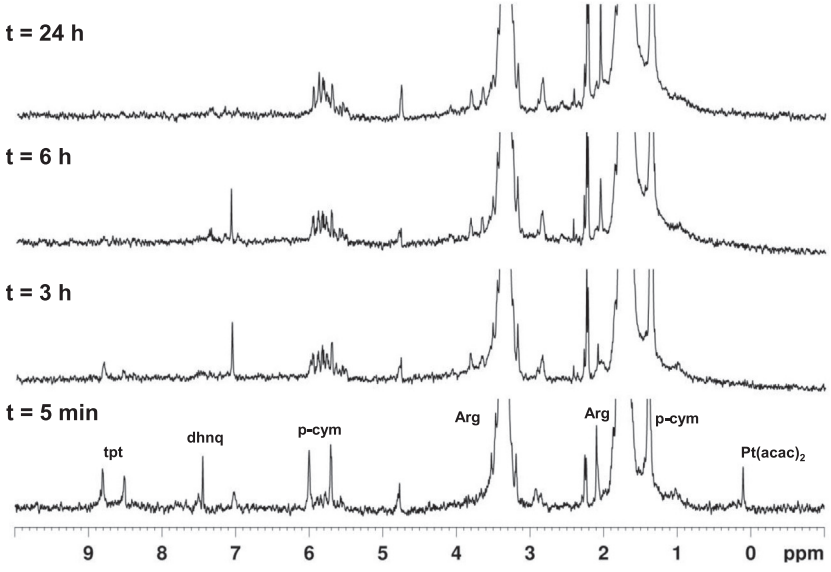

Fig. 2. ^1H NMR of the mixture $[Pt(acac)_2 \subset \mathbf{1}]^{6+}$/Arg (molar ratio 1:10) recorded at T = 37 °C, between t = 5 min and t = 24 h.

The structure of the chelate was confirmed with ESI mass spectrometry; peaks consistent with the complex $[(p\text{-cym})Ru(Arg)]^+$ and free Arg were identified at $m/z = 409.10$ and at $m/z = 175.12$, respectively (Table 1). However, as mentioned in previous reports [47,54] and although the ESI mass spectrum suggests the formation of $[(p\text{-cym})Ru(Arg)]^+$, the exact structure in solution cannot be determined, as coordination of additional water molecules cannot be ruled out.

Table 1
Peaks found in the ESI mass spectra of the mixtures $[Pt(acac)_2 \subset \mathbf{1}]^{6+}$/amino acids and $[Pt(acac)_2 \subset \mathbf{1}]^{6+}$/GSH.

Arg		His		Lys		Cys		GSH	
m/z	Species	*m/z*	Species	*m/z*	Species	*m/z*	Species	*m/z*	Species
175.12	Arg	156.08	His	147.11	Lys	241.03	cystine	313.12	tpt
313.12	tpt	313.12	tpt	313.12	tpt	313.12	tpt	394.06	$Pt(acac)_2$
409.10	$[(p\text{-cym})Ru\text{-}Arg]^+$	390.07	$[(p\text{-cym})Ru\text{-}His]^+$			356.03	$[(p\text{-cym})Ru\text{-}Cys]^+$	1015.73	$[\mathbf{1}](CF_3SO_3)_3^{3+}$
						394.06	$Pt(acac)_2$		

Figs. S3 and S4 show the ^{1}H NMR and DOSY NMR spectra obtained for the mixture [Pt(acac)$_2$⊂**1**]$^{6+}$ with His. As observed with the empty metallaprism [**1**]$^{6+}$ [42], the reaction was slower compared to Arg and reflects the difference in basicity between the two amino acid side chains. As noticed with [Pt(acac)$_2$⊂**2**]$^{6+}$ [47], the ^{1}H NMR resonances of Pt(acac)$_2$ between 0 and 4 ppm are no longer visible while the characteristic ^{1}H NMR resonances of the tpt, the dhnq and the *p*-cym moieties between 5.9 and 8 ppm are still present, suggesting that [**1**]$^{6+}$ did not react completely after 24 h. The fraction of [**1**]$^{6+}$ that reacted with His gave a chelate with the supposed formula [(*p*-cym)Ru(His)]$^+$, as described elsewhere [41–43,54]. The structure of this chelate could be further supported from the analysis of the ^{1}H NMR spectra, the DOSY spectra and also the ESI mass spectra (Table 1).

The new resonances adjacent to the resonances of *p*-cym (between 5 and 6 ppm and around 1 ppm) (Fig. S5) indicate that the kinetic of reaction of [Pt(acac)$_2$⊂**1**]$^{6+}$ with His was slower than the reaction of [**1**]$^{6+}$ with His. Indeed, the NMR spectra showed that the reaction was completed only after 72 h for [Pt(acac)$_2$⊂**1**]$^{6+}$ and after 24 h for [**1**]$^{6+}$.

This is again in contrast to the reactivity observed with [Pt(acac)$_2$⊂**2**]$^{6+}$ and [**2**]$^{6+}$, where the dismantling of both metallaprisms was complete within 24 h [42,47].

Upon addition of Lys, all resonances of [**1**]$^{6+}$ and of the encapsulated Pt(acac)$_2$ are still visible after 24 h, albeit at a lower intensity (Fig. S6). After 72 h, the reaction was completed. As expected, weak additional resonances near the resonances of free Lys between 1.5 and 3 ppm and near the resonances of the aromatic *p*-cym protons between 5.5 and 6 ppm gradually appeared, indicating the formation of the supposed chelate [(*p*-cym)Ru(Lys)]$^+$. Accordingly, the DOSY spectrum of the mixture exhibits three distinct components that correspond to [**1**]$^{6+}$, free Lys and the chelate [(*p*-cym)Ru(Lys)]$^+$ (Fig. S7). Similar to His and Arg, the respective NMR spectra recorded after 24 h clearly indicate that the reaction of [Pt(acac)$_2$⊂**1**]$^{6+}$ with Lys is much slower than the reaction of [**1**]$^{6+}$ with Lys (Fig. S8). However, this is once more in contrast to the reactivity observed with [Pt(acac)$_2$⊂**2**]$^{6+}$ and [**2**]$^{6+}$, the dismantling being almost instantaneous in both cases [42,47].

As Arg, His and Lys are present in the blood plasma with a concentration of 45, 68, and 148 mmol/L [58], respectively, these amino acids would be in very large excess compared to [Pt(acac)$_2$⊂**1**]$^{6+}$ if injected intravenously at its IC$_{50}$ concentration (Table 3). Hence, the robustness of [Pt(acac)$_2$⊂**1**]$^{6+}$ suggests that this water soluble metallaprism might be stable enough, and a large quantity should enter cells still intact with the encapsulated molecule inside the cavity, despite the presence of basic amino acids.

3.3. Interaction with Cys and GSH

Our previous investigations showed that hexacationic metallaprisms can catalyze the oxidation of Cys and GSH [41–43]. Notably, the increased autoxidation results from the presence of both the metallaprism and the triflate ions [41]. The ^{1}H NMR spectrum of the mixture [Pt(acac)$_2$⊂**1**]$^{6+}$/Cys (ratio 1:10) recorded after 24 h exhibits additional resonances, similar to those observed with the mixture [**1**]$^{6+}$/Cys [42], indicating that cystine is formed (Fig. 3 and Fig. S9). The oxidation of Cys was accompanied by the disassembly of [Pt(acac)$_2$⊂**1**]$^{6+}$ since the resonances of tpt and dhnq between 5.5 and 8 ppm were no longer visible. The 2D ^{1}H NMR DOSY spectrum clearly shows that both Cys and cystine were present in solution as well as fragments of [**1**]$^{6+}$ (Fig. S10). As observed with Arg and His, the rate of oxidation of Cys was similar with [Pt(acac)$_2$⊂**1**]$^{6+}$ and with [**1**]$^{6+}$. However, the dismantling of [**1**]$^{6+}$ was significantly slower than the dismantling of [Pt(acac)$_2$⊂**1**]$^{6+}$. The existence of degradation products was confirmed by the ESI mass spectrum (Table 1). In addition to free cystine and tpt, peaks corresponding to three different degradation products, at m/z = 356.03, which corresponds presumably to [(*p*-cym)Ru(Cys)]$^+$, and at m/z = 475.03 which corresponds to [(*p*-cym)Ru(cystine]$^+$.

Upon interaction of [Pt(acac)$_2$⊂**1**]$^{6+}$ with GSH, a rather limited oxidation of GSH to GSSG occurred and degradation of the metallaprism took place as indicated by the disappearance of the resonances for tpt, dhnq and Pt(acac)$_2$ in the ^{1}H NMR spectrum (Figs. S11 & S12). The reaction is similar to that reported for [**1**]$^{6+}$ but the rate of oxidation of GSH was much slower with [Pt(acac)$_2$⊂**1**]$^{6+}$ than with [**1**]$^{6+}$. The ESI mass spectrum suggests that no covalent interaction takes place (Table 1).

3.4. Reaction with proteins

Previously, we have established that electrostatic interactions between the empty metallaprisms [**1**]$^{6+}$, [**2**]$^{6+}$ [45], the complex-in-a-complex [Pt(acac)$_2$⊂**1**]$^{6+}$ [47] and the cytosolic proteins cytochrome *c* (Cyt c), myoglobin (Mb) and ubiquitin (Ub) as well as the two serum proteins human serum albumin (HsA) and transferrin (Tf) cause structural alterations of their secondary structure. The ^{1}H NMR spectra of the mixtures [Pt(acac)$_2$⊂**1**]$^{6+}$/HsA recorded over 96 h shown in Fig. 4 confirm this tendency. For both, the protein and [Pt(acac)$_2$⊂**1**]$^{6+}$, a general drop of the resonance's intensity is clear, suggesting that HsA and [Pt(acac)$_2$⊂**1**]$^{6+}$ precipitate from the reaction mixture. Precipitation is supported by the circular dichroism (CD) spectra: For the mixture [Pt(acac)$_2$⊂**1**]$^{6+}$/HsA, a reduction of the band intensity was observed compared to HsA alone (Fig. 5). As no band shifts were noticed, the observed changes in the CD bands seem to be due to the protein's precipitation and not a result of conformational changes as a result of the formation of soluble protein aggregates which are no longer chiral and therefore not active in circular dichroism spectroscopy, as shown by others [59], and reported for [Pt(acac)$_2$⊂**2**]$^{6+}$ [45]. Interestingly, the effect of the empty prism [**1**]$^{6+}$ on HsA was less pronounced than the effect of [Pt(acac)$_2$⊂**1**]$^{6+}$ as a strong CD band was still observed in the first case (Fig. 5). The CD spectrum suggests that HsA is still folded in a mostly α-helical structure in the presence of [**1**]$^{6+}$ [45,60]. Interestingly, the opposite effect was noticed with the smaller metallaprism [**2**]$^{6+}$: it appears that [**2**]$^{6+}$ precipitate more significantly than [Pt(acac)$_2$⊂**2**]$^{6+}$, suggesting that the reactivity of the filled metallaprism was lower than the empty one. As such, unlike amino acids, it appears that the larger metallaprism [Pt(acac)$_2$⊂**1**]$^{6+}$ has a stronger effect on the structure of HsA compared to the smaller metallaprism [Pt(acac)$_2$⊂**2**]$^{6+}$.

The ^{1}H NMR spectrum of the mixture [Pt(acac)$_2$⊂**1**]$^{6+}$/Tf shows a decrease of the intensity of the metallaprism's resonances over time likely due to precipitation of the [Pt(acac)$_2$⊂**1**]$^{6+}$ (Fig. S14). The intensity of the resonances of Tf slightly decreases as well, which can also be attributed to the precipitation of Tf. The intensity of the CD band decreased, suggesting precipitation or formation of aggregates (Fig. S18), as observed with [**1**]$^{6+}$ [45].

The NMR spectra of the mixture [Pt(acac)$_2$⊂**1**]$^{6+}$/Ub exhibited almost no changes over time (Fig. S15). As reported previously, no precipitation of Ub and of the empty metallaprisms [**1**]$^{6+}$ and [**2**]$^{6+}$ was observed [45], but significant changes in the respective NMR spectra were perceived with the complex-in-a-complex [Pt(acac)$_2$⊂**2**]$^{6+}$ [47].

The changes observed in the respective CD spectra were however more severe (Fig. S18). For Ub, no bands were observed in the presence of [Pt(acac)$_2$⊂**1**]$^{6+}$ suggesting again that Ub aggregates and losses chirality. Interestingly, for Ub, the effect of [Pt(acac)$_2$⊂**1**]$^{6+}$ on the structure of Ub is significantly larger than the effect of [**1**]$^{6+}$, as noticed for [Pt(acac)$_2$⊂**2**]$^{6+}$ which impose more significant changes in the structure of Ub than [**2**]$^{6+}$ [45,47].

The NMR spectra of the mixtures and [Pt(acac)$_2$⊂**1**]$^{6+}$/Cyt c exhibited almost no changes over time (Fig. S16), suggesting that

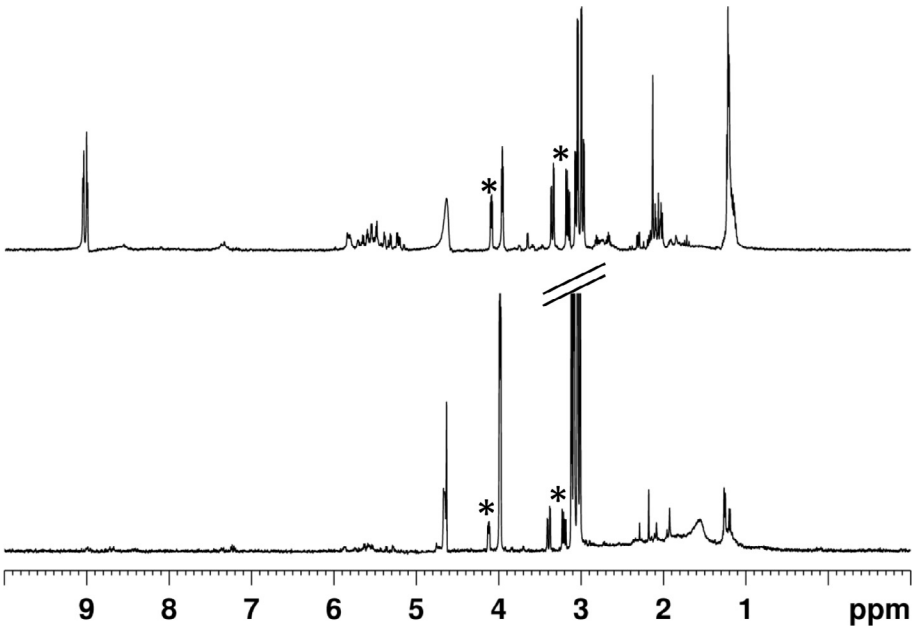

Fig. 3. Comparison of the ^{1}H NMR spectra of the mixture $[\mathbf{1}]^{6+}$/Cys (ratio 1:6) (top) and of the mixture $[Pt(acac)_2\subset\mathbf{1}]^{6+}$/Cys (ratio 1:10) (bottom). The resonances from the newly formed cystine are marked by (*).

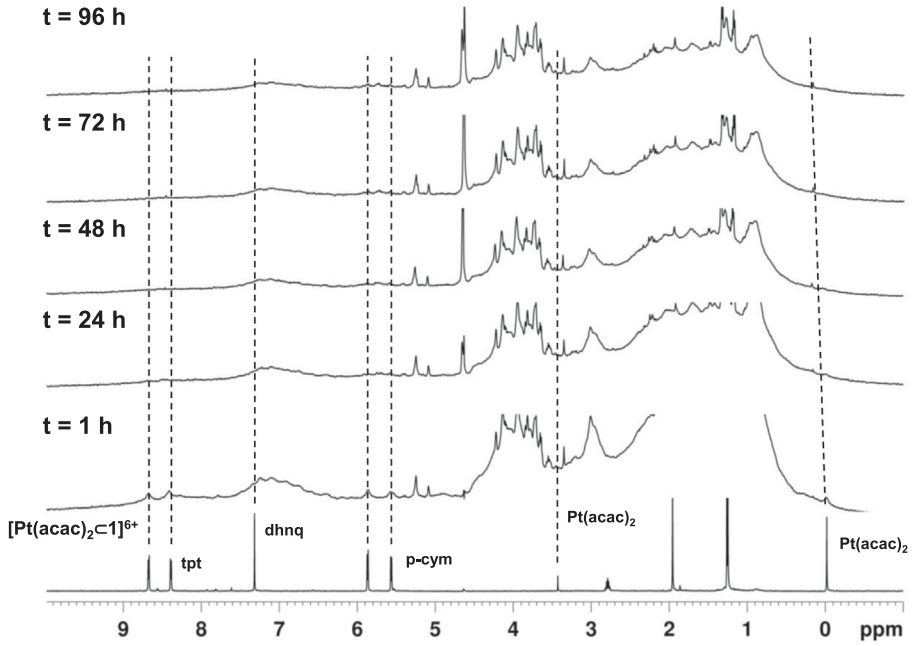

Fig. 4. ^{1}H NMR spectra of the mixture $[Pt(acac)_2\subset\mathbf{1}]^{6+}$/HsA (molar ratio 10:1) recorded between t = 1 h and t = 96 h. The ^{1}H NMR spectrum of $[Pt(acac)_2\subset\mathbf{1}]^{6+}$ is shown for comparison (bottom).

the two components do not interact, and that precipitation of Cyt c and the metallaprism takes place just to a very limited extent. This behavior is similar to the observation made with $[Pt(acac)_2\subset\mathbf{2}]^{6+}$ [47], but in contrast to both empty metallaprisms $[\mathbf{1}]^{6+}$ and $[\mathbf{2}]^{6+}$ for which important precipitation of Cyt c and the respective metallaprism was noticed [45]. However, similar to $[Pt(acac)_2\subset\mathbf{2}]^{6+}$, $[Pt(acac)_2\subset\mathbf{1}]^{6+}$ also induces strong structural effects on the structure of Cyt c, as a complete disappearance of the CD band was observed (Fig. S18). Soluble aggregates of Cyt c seem to be formed that are no longer chiral and therefore not active in CD spectrometry (Fig. S18) [45,47].

The ^{1}H NMR spectra of the mixture $[Pt(acac)_2\subset\mathbf{1}]^{6+}$/Mb showed a decrease of the overall intensity coupled to a line broadening of the resonances of Mb. These effects can be attributed to aggregation (Fig. S17). The CD spectrum shows no bands for Mb upon interaction with $[Pt(acac)_2\subset\mathbf{1}]^{6+}$ (Fig. S18). The strong aggregation of the protein induced by the presence of the $[Pt(acac)_2\subset\mathbf{1}]^{6+}$ could account for the absence of bands in the CD spectrum [45]. Interestingly, as observed with Ub, the structural effects imposed by $[Pt(acac)_2\subset\mathbf{1}]^{6+}$ on the structure of Mb are much stronger than the effects imposed by the empty metallaprism $[\mathbf{1}]^{6+}$.

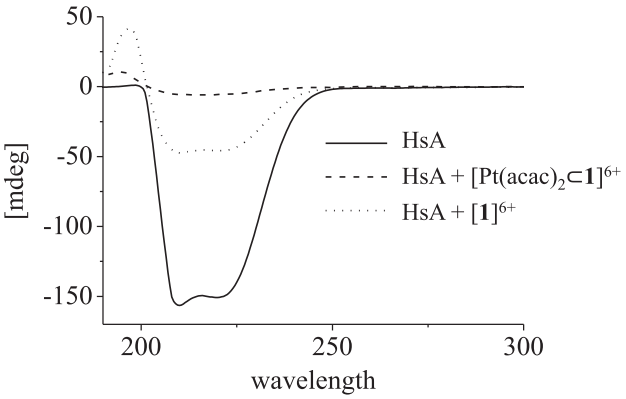

Fig. 5. CD spectra of HsA alone and in the presence of the metallaprisms [Pt(acac)$_2$⊂**1**]$^{6+}$ and [**1**]$^{6+}$. The reduction of the band intensity is caused by the precipitation of HsA.

MALDI-TOF mass spectra performed in the negative mode confirm the electrostatic nature of the interactions between [Pt(acac)$_2$⊂**1**]$^{6+}$ and the proteins. As observed for [Pt(acac)$_2$⊂**2**]$^{6+}$ [47], no fragments that would prove the formation of adducts between the proteins and [Pt(acac)$_2$⊂**1**]$^{6+}$ were identified.

In conclusion, the structural alterations imposed by [Pt(acac)$_2$⊂**1**]$^{6+}$ on the proteins appear stronger compared to those imposed by [**1**]$^{6+}$, as observed for [Pt(acac)$_2$⊂**2**]$^{6+}$ which imposes stronger changes compared to [**2**]$^{6+}$ [47]. It turns out that in the presence of [Pt(acac)$_2$⊂**1**]$^{6+}$ and [Pt(acac)$_2$⊂**2**]$^{6+}$, the formation of protein aggregates is increased which results in the complete disappearing of the CD bands. An explanation of this phenomenon might be found in the different structure of the filled and empty metallaprism as described elsewhere [36,47].

3.5. Reaction with nucleotides

The ^{1}H NMR and the 2D DOSY NMR spectra of the mixtures [Pt(acac)$_2$⊂**1**]$^{6+}$/nuc, nuc = dGMP, dAMP, dCMP or dTMP are shown in Figs. S19–S26. Similarly to what we have observed for [**1**]$^{6+}$ [44], none of the ^{1}H NMR spectra exhibited any additional resonances, neither the DOSY NMR spectra suggest the presence of other species than [Pt(acac)$_2$⊂**1**]$^{6+}$ and the free nucleotide. The ESI mass spectra corresponding to these mixtures are summarized in Table 2. Only peaks corresponding to the free nucleotides and fragments of [Pt(acac)$_2$⊂**1**]$^{6+}$ were identified. These results parallel those obtained with the smaller, more reactive metallaprisms [**2**]$^{6+}$ and [Pt(acac)$_2$⊂**2**]$^{6+}$: in both cases only a slow and incomplete reaction with dGMP was observed [43,47].

3.6. Reaction with the dodecamer d(CGCGATCGCG)$_2$

Fig. S27 shows the ^{1}H NMR spectra of the mixture of [Pt(acac)$_2$⊂**1**]$^{6+}$/dodecamer d(CGCGATCGCG)$_2$ in D_2O with addition of 0.01% NaN_3 and 10 mM Na_2HPO_4/KH_2PO_4 to stabilize the oligomer. No significant changes were observed over 96 h, strongly suggesting that no covalent interactions between [Pt(acac)$_2$⊂**1**]$^{6+}$ and the dodecamer d(CGCGATCGCG)$_2$ took place.

The CD spectra recorded on the mixture [Pt(acac)$_2$⊂**1**]$^{6+}$/d(CGCGATCGCG)$_2$ (ratio 1:1) over a period of 48 h are shown in Fig. 6. The decrease of the CD bands in the spectra of d(CGCGATCGCG)$_2$ over time indicates an unwinding of the double strand, as observed with the smaller metallaprism [Pt(acac)$_2$⊂**2**]$^{6+}$ [44]. Notably, the CD spectra of the mixtures [Pt(acac)$_2$⊂**1**]$^{6+}$/d(CGCGATCGCG)$_2$ and [**1**]$^{6+}$/d(CGCGATCGCG)$_2$ (Fig. S28) exhibit only marginal differences, suggesting that electrostatic interactions between the positively charged [Pt(acac)$_2$⊂**1**]$^{6+}$ and [**1**]$^{6+}$ and the negatively charged backbone of d(CGCGATCGCG)$_2$ impose similar structural changes.

The mixture [Pt(acac)$_2$⊂**1**]$^{6+}$/ d(CGCGATCGCG)$_2$ was subsequently monitored by UV/Vis spectroscopy (Figs. S29–S31). As observed with [Pt(acac)$_2$⊂**2**]$^{6+}$ [47] and [**1**]$^{6+}$ [44], the bands for the mixture [Pt(acac)$_2$⊂**1**]$^{6+}$/d(CGCGATCGCG)$_2$ are of higher intensity than the sum of the individual bands, suggesting that [Pt(acac)$_2$⊂**1**]$^{6+}$ causes unwinding of the oligomer d(CGCGATCGCG)$_2$ as well. Due to the band overlap, a quantitative evaluation for the unwinding of the oligomer was not possible. The decrease of the UV/Vis bands corresponding to [Pt(acac)$_2$⊂**1**]$^{6+}$ might be attributed to the precipitation or decomposition of the metallaprism due to the presence of NaN_3 in solution [44,47].

ESI mass spectra in both the positive and negative mode of d(CGCGATCGCG)$_2$ alone and of the mixture [Pt(acac)$_2$⊂**1**]$^{6+}$/d(CGCGATCGCG)$_2$ were recorded. Under a negative mode, no peaks that would indicate the formation of adducts between the metallaprism [**1**]$^{6+}$ or Pt(acac)$_2$ and d(CGCGATCGCG)$_2$ were found (Fig. S32), as previously found for [Pt(acac)$_2$⊂**2**]$^{6+}$ [47]. The spectra recorded in the positive mode did not reveal peaks that would indicate the formation of an adduct between [Pt(acac)$_2$⊂**1**]$^{6+}$ and d(CGCGATCGCG)$_2$ (Fig. S33).

The results obtained from NMR, MS, CD and UV/Vis clearly suggest that only electrostatic interactions take place between [Pt(acac)$_2$⊂**1**]$^{6+}$ and d(CGCGATCGCG)$_2$, thus leading to the unwinding of the double helix. The results are in accordance with those reported previously and indicate a similar reactivity for [**1**]$^{6+}$ and the complex-in-a-complex [Pt(acac)$_2$⊂**1**]$^{6+}$ [44]. In addition, no evidence of a direct interaction between d(CGCGATCGCG)$_2$ and Pt(acac)$_2$ was found.

3.7. Relationship cytotoxicity - reactivity

In order to evaluate the cytotoxicity of [Pt(acac)$_2$⊂**1**]$^{6+}$, we determined the *in vitro* activity on cancerous, human ovarian cancer cells A2780 and their cisplatin resistant mutant A2780cisR, and on the non-cancerous human embryonic kidney cells HEK-293. These IC_{50} values are compared to those obtained for [**1**]$^{6+}$ and cisplatin (Table 3).

Both [Pt(acac)$_2$⊂**1**]$^{6+}$ and [**1**]$^{6+}$ are significantly more cytotoxic than cisplatin with IC_{50} values in the low micromolar range, but show no selectivity towards cancer cells. Interestingly, the general inverse correlation between the cytotoxicity and the reactivity usually observed for metal-based drugs, as suggested by Hartinger and coworkers [46] and observed for thiolato bridged arene

Table 2
Summary of peaks found in the ESI mass spectra of the mixtures [Pt(acac)$_2$⊂**1**]$^{6+}$/nucleotides.

dAMP		dGMP		dCMP		dTMP	
m/z	Species	*m/z*	Species	*m/z*	Species	*m/z*	Species
313.12	tpt	313.12	tpt	308.06	dCMP	313.12	tpt
332.07	dAMP	1016.40	[**1**](CF$_3$SO$_3$)$_3^{3+}$	1016.40	[**1**](CF$_3$SO$_3$)$_3^{3+}$	367.03	dTMP
1016.40	[**1**](CF$_3$SO$_3$)$_3^{3+}$					1016.40	[**1**](CF$_3$SO$_3$)$_3^{3+}$

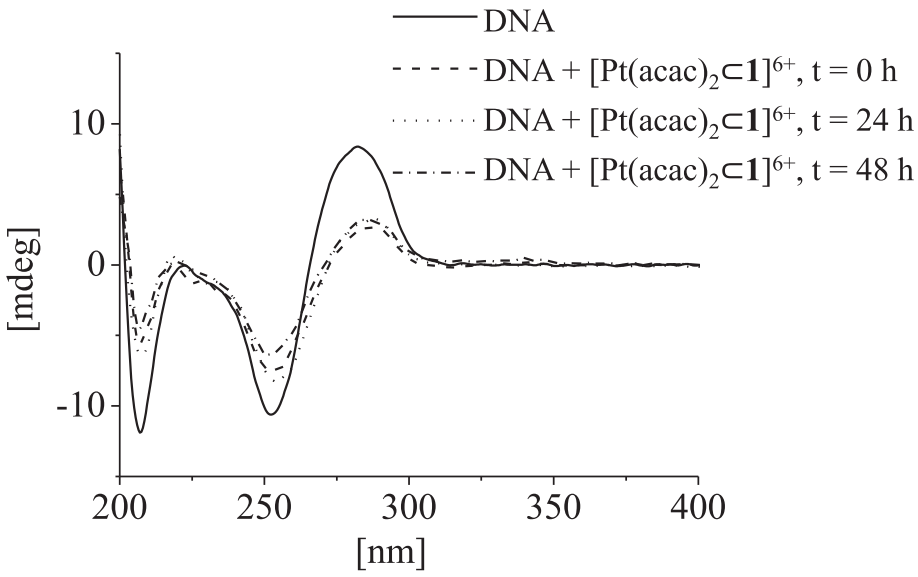

Fig. 6. CD spectra of the mixture $[Pt(acac)_2\subset\mathbf{1}]^{6+}$/d(CGCGATCGCG)$_2$ (ratio 1:1) and of d(CGCGATCGCG)$_2$ alone recorded between t = 0 h and t = 48 h.

Table 3
IC_{50} values of the metallaprisms $[Pt(acac)_2\subset\mathbf{1}]^{6+}$ and $[\mathbf{1}]^{6+}$ and cisplatin against three different cell lines determined with Dojindo Cell Counting Kit 8.

	A2780	A2780cisR	HEK293
$[Pt(acac)_2\subset\mathbf{1}]^{6+}$	0.12 ± 0.01	0.47 ± 0.06	0.18 ± 0.03
$[\mathbf{1}]^{6+}$	0.45 ± 0.07	0.42 ± 0.01	0.22 ± 0.01
cisplatin	2.94 ± 0.17	21.90 ± 0.80	86.67 ± 23.11

ruthenium complexes [61], is only partly true for these metallaprisms. Indeed, $[Pt(acac)_2\subset\mathbf{1}]^{6+}$ is slightly more cytotoxic than $[\mathbf{1}]^{6+}$ against A2780 cells but equally cytotoxic against both A2780-cisR and HEK-293 cells. However, $[Pt(acac)_2\subset\mathbf{1}]^{6+}$ reacts slowly than $[\mathbf{1}]^{6+}$ towards amino acids, reacts similarly towards a dodecamer, but imposes stronger changes in the structure of proteins.

4. Conclusions

The encapsulation of $Pt(acac)_2$ in the large metallaprism $[\mathbf{1}]^{6+}$ to form the complex-in-a-complex $[Pt(acac)_2\subset\mathbf{1}]^{6+}$ slightly increases its *in vitro* cytotoxicity against the cell line A2780, but not against the cell lines A2780cisR and HEK293. This is in contrast to the smaller metallaprism $[Pt(acac)_2\subset\mathbf{2}]^{6+}$: The *in vitro* cytotoxicity could be reduced by a factor ten compared to the empty metallaprism $[\mathbf{2}]^{6+}$ [36], and might be tentatively related to the increased stability of $[Pt(acac)_2\subset\mathbf{1}]^{6+}$ towards biomolecules compared to $[Pt(acac)_2\subset\mathbf{2}]^{6+}$. To this end, the study of the stability and the reactivity of $[Pt(acac)_2\subset\mathbf{1}]^{6+}$ towards model biomolecules represented an important step for understanding the properties and capabilities of this metallaprism.

More specifically, our results showed that $[Pt(acac)_2\subset\mathbf{1}]^{6+}$ reacts to a limited extent and much slowly than $[\mathbf{1}]^{6+}$ [42] and especially than $[Pt(acac)_2\subset\mathbf{2}]^{6+}$ [47] with amino acids, while the same degradation products are formed. In the presence of proteins, electrostatic interactions lead to significant changes in the secondary structure of HsA, Tf, and Mb, while the structures of Cyt c and Ub seem to be unaffected. The structural changes imposed on the proteins are however more pronounced than with $[\mathbf{1}]^{6+}$ and are accompanied by precipitation of the proteins and $[Pt(acac)_2\subset\mathbf{1}]^{6+}$. An explanation of this phenomenon might be found in the different structure of the filled and empty metallaprism [36,47]. As $[\mathbf{1}]^{6+}$, $[Pt(acac)_2\subset\mathbf{1}]^{6+}$ did not covalently bind to the oligonucleotide d(CGCGATCGCG)$_2$ but electrostatic interactions cause unwinding of the double strand.

Overall, the results obtained in this study with $[Pt(acac)_2\subset\mathbf{1}]^{6+}$ are in agreement with our previous study that compared the smaller complex-in-a-complex $[Pt(acac)_2\subset\mathbf{2}]^{6+}$ with its empty counterpart $[\mathbf{2}]^{6+}$: When a guest molecule is trapped in the cavity of the metallaprism, the reactivity towards amino acids and nucleotides is reduced, the reactivity towards DNA remains similar, while stronger effects are imposed on the secondary structure of several cytosolic and plasma proteins.

Following the tendency observed with the empty metallaprisms, $[Pt(acac)_2\subset\mathbf{1}]^{6+}$ is more robust than $[Pt(acac)_2\subset\mathbf{2}]^{6+}$ and may remain intact in the bloodstream and, therefore, may enter cancer cells undamaged, thus confirming the drug delivery potential for this water-soluble organometallic prism.

Acknowledgments

J. F. thanks the Swiss National Science Foundation (Grant No 206021_139078) for financial support. A generous loan of ruthenium chloride hydrate from the Johnson Matthey Technology Center is gratefully acknowledged.

Appendix A. Supplementary data

Supplementary data associated with this article can be found, in the online version, at http://dx.doi.org/10.1016/j.ica.2017.08.045.

References

[1] G. Jaouen, W. Beck, M.J. McGlinchey, A Novel Field of Research: Bioorganometallic Chemistry, Origins, and Founding Principles, Bioorganometallics, Wiley-VCH Verlag GmbH & Co. KGaA, 2006, p. 1.
[2] J. Furrer, G.S. Smith, B. Therrien, Metal Complexes as Enzyme Inhibitors and Catalysts in Living Cells, Inorganic Chemical Biology, John Wiley & Sons, Ltd, 2014, p. 341.
[3] B. Rosenberg, L. Van Camp, T. Krigas, Nature 205 (1965) 698.
[4] K.D. Mjos, C. Orvig, Chem. Rev. (Washington, DC, U. S.) 114 (2014) 4540.
[5] N.J. Wheate, S. Walker, G.E. Craig, R. Oun, Dalton Trans. 39 (2010) 8113.
[6] N.J. Wheate, J.G. Collins, Coord. Chem. Rev. 241 (2003) 133.
[7] M.J. Clarke, F. Zhu, D.R. Frasca, Chem. Rev. 99 (1999) 2511.
[8] K.D. Mjos, C. Orvig, Chem. Rev. 114 (2014) 4540.
[9] G. Süss-Fink, Dalton Trans. 39 (2010) 1673.

[10] A. Bergamo, G. Sava, Dalton Trans. 2007 (2007) 1267.
[11] I. Bratsos, S. Jedner, T. Gianferrara, E. Alessio, Chimia 61 (2007) 692.
[12] C.G. Hartinger, M.A. Jakupec, S. Zorbas-Seifried, M. Groessl, A. Egger, W. Berger, H. Zorbas, P.J. Dyson, B.K. Keppler, Chem. Biodiversity 5 (2008) 2140.
[13] R. Trondl, P. Heffeter, C.R. Kowol, M.A. Jakupec, W. Berger, B.K. Keppler, Chem. Sci. 5 (2014) 2925.
[14] G. Gasser, I. Ott, N. Metzler-Nolte, J. Med. Chem. 54 (2011) 3.
[15] R.E. Morris, R.E. Aird, P. del Socorro Murdoch, H. Chen, J. Cummings, N.D. Hughes, S. Parsons, A. Parkin, G. Boyd, D.I. Jodrell, P.J. Sadler, J. Med. Chem. 44 (2001) 3616.
[16] K.S.M. Smalley, R. Contractor, N.K. Haass, A.N. Kulp, G.E. Atilla-Gokcumen, D.S. Williams, H. Bregman, K.T. Flaherty, M.S. Soengas, E. Meggers, M. Herlyn, Cancer Res. 67 (2007) 209.
[17] A. Bergamo, C. Gaiddon, J.H.M. Schellens, J.H. Beijnen, G. Sava, J. Inorg. Biochem. 106 (2012) 90.
[18] A.-L. Lainé, C. Passirani, Curr. Opin. Pharmacol. 12 (2012) 420.
[19] G. Tiwari, R. Tiwari, B. Sriwastawa, L. Bhati, S. Pandey, P. Pandey, S.K. Bannerjee, Int. J. Pharma. Invest. 2 (2012) 2.
[20] W.H. De Jong, P.J.A. Borm, Int. J. Nanomed. 3 (2008) 133.
[21] A. Lavasanifar, J. Samuel, G.S. Kwon, Adv. Drug Deliv. Rev. 54 (2002) 169.
[22] M. Alagusundaram, C.M.S. Chetty, K. Umashankari, V.B. Attuluri, C. Lavanya, S. Ramkanth, Int. J. ChemTech Res. 1 (2009) 526.
[23] A. Samad, Y. Sultana, M. Aqil, Curr. Drug Delivery 4 (2007) 297.
[24] E. Quartapelle Procopio, S. Rojas, N.M. Padial, S. Galli, N. Masciocchi, F. Linares, D. Miguel, J.E. Oltra, J.A.R. Navarro, E. Barea, Chem. Commun. 47 (2011) 11751.
[25] P. Govender, B. Therrien, G.S. Smith, Eur. J. Inorg. Chem. 2012 (2012) 2853.
[26] F. Arnesano, G. Natile, Coord. Chem. Rev. 253 (2009) 2070.
[27] K. Ajima, M. Yudasaka, T. Murakami, A. Maigné, K. Shiba, S. Iijima, Mol. Pharm. 2 (2005) 475.
[28] R.P. Feazell, N. Nakayama-Ratchford, H. Dai, S.J. Lippard, J. Am. Chem. Soc. 129 (2007) 8438.
[29] M. Fujita, M. Tominaga, A. Hori, B. Therrien, Acc. Chem. Res. 38 (2005) 369.
[30] S. Leininger, B. Olenyuk, P.J. Stang, Chem. Rev. (Washington, DC, U. S.) 100 (2000) 853.
[31] S.R. Seidel, P.J. Stang, Acc. Chem. Res. 35 (2002) 972.
[32] B. Therrien, Top. Curr. Chem. 319 (2012) 35.
[33] T.B. Rauchfuss, K. Severin, Supramolecular architectures based on organometallic half-sandwich complexes, in: J.L. Atwood, J.W. Steed (Eds.), Organic Nanostructures, Wiley-VCH, 2008, p. 179.
[34] B. Therrien, Eur. J. Inorg. Chem. (2009) 2445.
[35] B. Therrien, Drug delivery by water-soluble organometallic cages, in: M. Albrecht, E. Hahn (Eds.), Chemistry of Nanocontainers, Springer Berlin Heidelberg, Berlin, Heidelberg, 2012, p. 35.
[36] B. Therrien, G. Süss-Fink, P. Govindaswamy, A.K. Renfrew, P.J. Dyson, Angew. Chem., Int. Ed. Engl. 47 (2008) 3773.
[37] J. Mattsson, P. Govindaswamy, J. Furrer, Y. Sei, K. Yamaguchi, G. Suess-Fink, B. Therrien, Organometallics 27 (2008) 4346.
[38] J. Mattsson, O. Zava, A.K. Renfrew, Y. Sei, K. Yamaguchi, P.J. Dyson, B. Therrien, Dalton Trans. 39 (2010) 8248.
[39] O. Zava, J. Mattsson, B. Therrien, P.J. Dyson, Chem. –Eur. J. 16 (2010) 1428.
[40] B. Therrien, G. Suess-Fink, P. Govindaswamy, A.K. Renfrew, P.J. Dyson, Angew. Chem., Int. Ed. Engl. 47 (2008) 3773.
[41] L.E.H. Paul, J. Furrer, B. Therrien, J. Organomet. Chem. 734 (2013) 45.
[42] L.E.H. Paul, B. Therrien, J. Furrer, J. Biol. Inorg. Chem. 17 (2012) 1053.
[43] L.E.H. Paul, B. Therrien, J. Furrer, Inorg. Chem. 51 (2012) 1057.
[44] L.E.H. Paul, B. Therrien, J. Furrer, J. Biol. Inorg. Chem. 20 (2015) 49.
[45] L.E.H. Paul, B. Therrien, J. Furrer, Org. Biomol. Chem. 13 (2015) 946.
[46] S.M. Meier, M. Hanif, W. Kandioller, B.K. Keppler, C.G. Hartinger, J. Inorg. Biochem. 108 (2012) 91.
[47] L.E.H. Paul, B. Therrien, J. Furrer, J. Organomet. Chem. 796 (2015) 39.
[48] A. Myari, N. Hadjiliadis, A. Garoufis, J. Malina, V. Brabec, J. Biol. Inorg. Chem. 12 (2007) 279.
[49] E.M. Proudfoot, J.P. Mackay, P. Karuso, Biochemistry 40 (2001) 4867.
[50] J.D. Watson, F.H.C. Crick, Nature 171 (1953) 737.
[51] N.P.E. Barry, B. Therrien, Eur. J. Inorg. Chem. (2009) 4695.
[52] L. Biro, E. Farkas, P. Buglyo, Dalton Trans. 39 (2010) 10272.
[53] L. Biro, E. Farkas, P. Buglyo, Dalton Trans. 41 (2012) 285.
[54] F.A. Egbewande, L.E.H. Paul, B. Therrien, J. Furrer, Eur. J. Inorg. Chem. (2014) 1174.
[55] K.F. Morris, C.S. Johnson, J. Am. Chem. Soc. 114 (1992) 3139.
[56] G.A. Morris, Diffusion-ordered spectroscopy (DOSY), in: D.M. Grant, R.K. Harris (Eds.), Encyclopedy of Nuclear Magnetic Resonance, Wiley, 2002, p. 35.
[57] R. Krämer, M. Maurus, R. Bergs, K. Polborn, K. Sünkel, B. Wagner, W. Beck, Chem. Ber. 126 (1993) 1969.
[58] A. Canepa, J.C.D. Filho, A. Gutierrez, A. Carrea, A.M. Forsberg, E. Nilsson, E. Verrina, F. Perfumo, J. Bergström, Nephrol. Dial. Transplant. 17 (2002) 413.
[59] S.M. Kelly, T.J. Jess, N.C. Price, Biochim. Biophys. Acta Proteins Proteomics 1751 (2005) 119.
[60] S.M. Kelly, N.C. Price, Curr. Protein Pept. Sci. 1 (2000) 349.
[61] J. Furrer, G. Süss-Fink, Coord. Chem. Rev. 309 (2016) 36.